S. C. Kacker

Staff Aerodynamicist.
Pratt & Whitney Aircraft of Canada Ltd.,

U. Okapuu

Chief, Turbine Aerodynamics.

Pratt & Whitney Aircraft of Canada Ltd.,
Longueuil, Quebec, Canada

A Mean Line Prediction Method for Axial Flow Turbine Efficiency

A mean line loss system is described, capable of predicting the design point efficiencies of current axial turbines of gas turbine engines. This loss system is a development of the Ainley/Mathieson technique of 1951. The prediction method is tested against the "Smith's chart" and against the known efficiencies of 33 turbines of recent design. It is shown to be able to predict the efficiencies of a wide range of axial turbines of conventional stage loadings to within ± 1½ percent.

Introduction

In choosing the gas path for a new turbine the designer has to carry out an optimization study which involves the calculation of velocity triangles. Blade lengths and radii are thereby determined early in the design cycle, before blade shapes are known. This is done by means of a "mean line" velocity triangle calculation, which is based on the assumption that the thermodynamic processes undergone by the working fluid can be represented by velocity triangles at midspan. To produce an optimum gas path such a calculation must incorporate a system of aerodynamic losses expressed as a function of blade row inlet and exit velocity triangles. Its excellence is ultimately judged by its ability to predict the aerodynamic efficiencies of known turbines of "competent" design.

Over the past 30 yr, a number of such turbine mean line loss systems have been described in the open literature, Traupel [1], Craig and Cox [2], and Stewart [3]. Perhaps the best known and most completely documented of these is that due to Ainley and Mathieson [4], published in 1951. Due to the improvement in our analytical capability and the accumulation of test results on a variety of turbines, it is fitting that such a loss system be critically reviewed and updated at least once every decade. It is a tribute to the durability of the Ainley/Mathieson system that it has become a foundation worthy of subsequent refinement, the most notable of which was published in 1970 by Dunham and Came [5]. Now, a decade later, may be an appropriate time to take a fresh look at the subject.

The present paper describes modifications to the Ainley/Mathieson/Dunham/Came (AMDC) loss system. These modifications are tested against experimental results where possible. The complete loss system is finally tested against design point efficiencies of 33 recent turbines.

Overall Description of Loss System

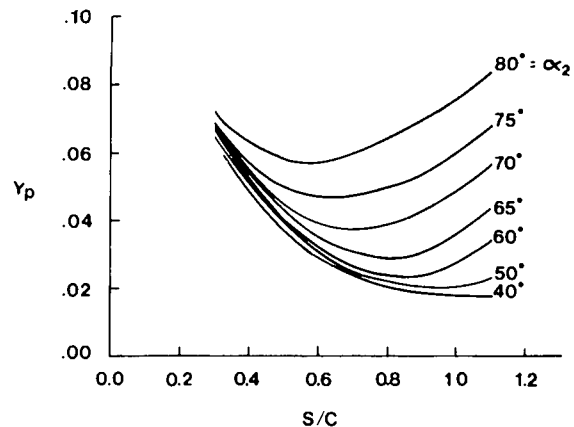The loss of total pressure in a cascade of blades, expressed

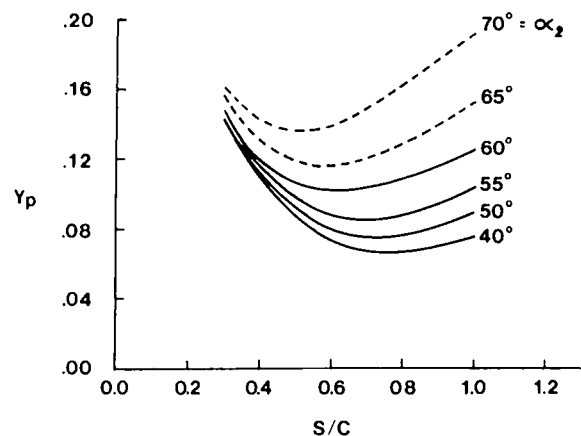**Fig. 1** Profile loss coefficient for $\beta_1 = 0$, $t_{MAX}/c = 0.2$ after Ainley and Mathieson [4]

Fig. 2 Profile loss coefficient for $\beta_1 = \alpha_2$, $t_{MA}/c = 0.2$ after Ainley and Mathieson [4]

in terms of cascade exit dynamic pressure, is assumed to be the sum of profile, secondary, trailing edge and tip leakage losses, where the profile losses are corrected for Reynolds' number effects
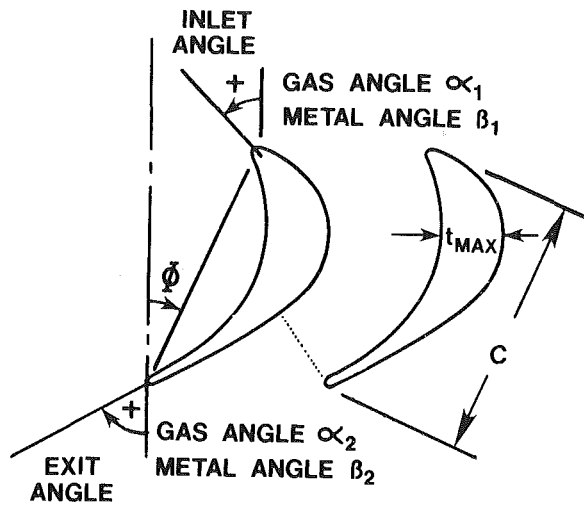
Fig. 3 Blade section terminology

Fig. 4 Thickness/chord ratio for typical turbine blade sections

$$Y_T = Y_P f_{(Re)} + Y_s + Y'_{TET} + Y_{TC} \tag{1}$$

This formulation is seen to differ from that of the AMDC system [4, 5], which is

$$Y_T = [(Y_P + Y_S)\text{REFAC} + Y_{TC}]Y_{TET} \tag{2}$$

where Y_{TET} in Equ. (2) is a multiplier, not a loss coefficient.

In equation (1), blade Reynolds' number is taken to affect only the profile loss coefficient, and the trailing edge loss coefficient is separated from the other loss terms. This would appear a more logical arrangement, since it is difficult to justify a connection between trailing edge losses and tip clearance losses, for example.
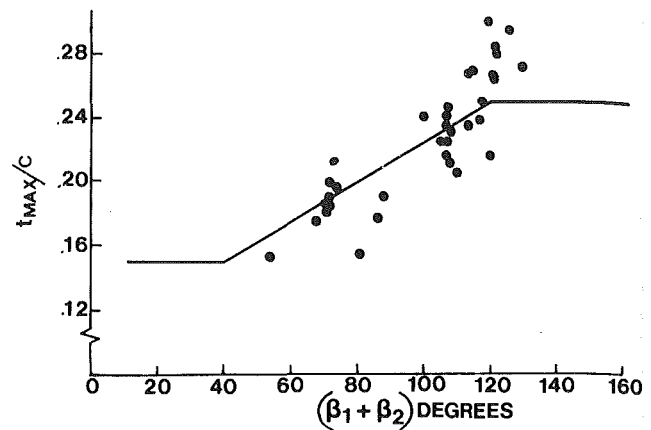
The Profile Loss Coefficient Y_P

The basis for the profile loss coefficient is a set of cascade test results incorporated in the AMDC loss system [4]. These results are expressed in terms of pitch/chord ratio and cascade exit gas angle α_2 for two special cases of $\beta_1 = 0$ (Fig. 1) and $\beta_1 = \alpha_2$ (Fig. 2). For any other combination of angles, these graphs are interpolated by means of the following equation:

$$Y_{P,\text{AMDC}} = \left\{ Y_{P(\beta_1 = 0)} + \left| \frac{\beta_1}{\alpha_2} \right| \left(\frac{\beta_1}{\alpha_2} \right) \left[Y_{P(\beta_1 = \alpha_2)} \right. \right.$$
$$\left. \left. - Y_{P(\beta_1 = 0)} \right] \right\} \left(\frac{t_{\text{MAX}}/c}{0.2} \right)^{\frac{\beta_1}{\alpha_2}} \tag{3}$$

The foregoing equation is similar to the interpolation

--- Nomenclature ---

b_x	=	axial chord
C	=	true chord
C_L	=	airfoil lift coefficient
C_x	=	axial velocity component
CFM	=	supersonic drag rise multiplying factor to profile loss coefficient Y_P
$f_{(AR)}$	=	aspect ratio function
$f_{(Re)}$	=	Reynolds number correction factor
h	=	blade or vane height
ΔH	=	enthalpy drop
k	=	tip clearance
k'	=	equivalent tip clearance for shrouded blade
K_1, K_2, K_3, K_p, K_s	=	correction factors defined in text
M	=	Mach number
o	=	throat opening
P	=	total pressure
p	=	static pressure
q	=	dynamic head ($P-p$)
REFAC	=	Reynolds number correction factor for AMDC loss system
Rec	=	Reynolds number based on true chord and exit gas conditions
R	=	radius
s	=	pitch
U	=	blade velocity at mid height
t	=	trailing edge thickness (TET)
t_{MAX}	=	blade maximum thickness
Y	=	loss coefficient $\Delta P/q$ where q is (generally) taken at blade exit

Y_T	=	total loss coefficient for a blade row
Y_P	=	profile loss coefficient
Y_S	=	secondary loss coefficient
Y_{SHOCK}	=	component of profile loss coefficient due to leading edge shock
Y_{TET}	=	trailing edge loss multiplier, in AMDC loss system
Y'_{TET}	=	trailing edge loss coefficient
Y_{TC}	=	tip clearance loss coefficient
α	=	absolute/relative gas angles for vane/blade
α_m	=	mean gas angle defined in equation (13)
β	=	metal angle for vane or blade
γ	=	ratio of specific heats
$\Delta\phi^2{}_{\text{TET}}$	=	trailing edge K.E. loss coefficient
η_{t-t}	=	turbine efficiency (total-to-total)
η_o	=	η_{t-t} at zero tip clearance
Φ	=	stagger angle
ϕ^2	=	kinetic energy coefficient = (actual gas exit velocity/ideal gas exit velocity)^2

Subscripts

H	=	hub
T	=	tip
1,2	=	inlet and exit conditions
Sub	=	subsonic
AMDC	=	as per Ainley, Mathieson, Dunham and Came
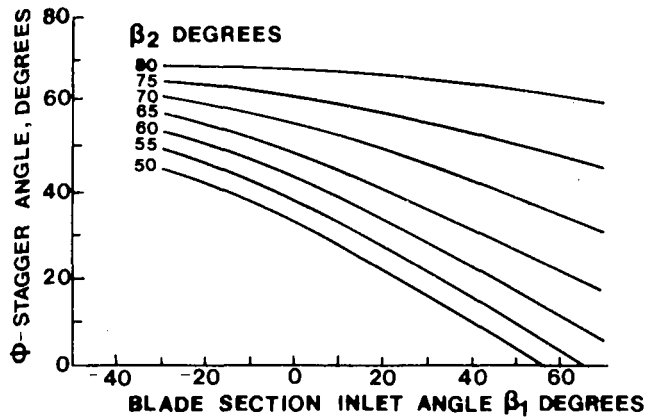
Fig. 5 Stagger angle for typical turbine blade sections

Fig. 6 Inlet Mach number ratio for nonfree-vortex turbine blades
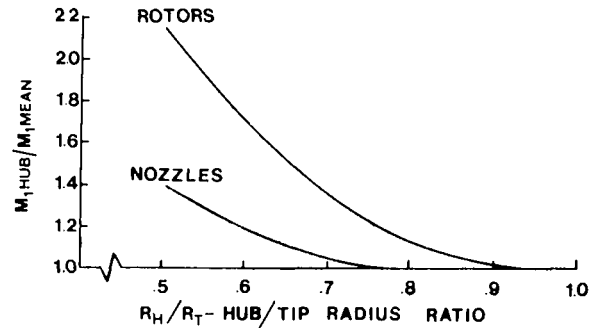

Fig. 7 Combined effect of leading edge shock on inner end wall flow and the blade channel next to it

equation given by the AMDC method except for the term $|\beta_1/\alpha_2|$, which was introduced to allow for negative inlet angle.

Figure 3 clarifies the terminology. Figure 4, a plot of thickness/chord ratios of a number of recent blade designs, proposes a general curve for this ratio, to be used when blade sections are not yet designed. Figure 5, similarly of statistical derivation, proposes values of stagger angle which can be used to estimate true chords, c, from axial chords which are generally established early in the design.

The cascade results of Figs. 1 and 2 are valid for vanes and blades having a trailing edge thickness to pitch ratio (t/s) of 0.02. In the AMDC loss system Y_p is multiplied by Y_{TET} to obtain the combined profile and trailing edge loss at any other t/s ratio. In the present loss system, since Y'_{TET} is a separate additive loss, Y_p from Figs. 1 and 2 is multiplied by 0.914, which is the value of Y_{TET} at $t/s = 0$ according to AMDC loss system, to obtain Y_p at zero trailing edge thickness.

The AMDC profile loss correlations, Figs. 1 and 2, were perfectly valid at the time of publication of the original AMDC loss system, and efficiencies of turbines of that era should be predictable by these data. However, advances in aerodynamic analysis, made over the last three decades, suggest that a factor of 2/3 should be applied to these loss coefficients for the efficiency prediction of present-day turbines.

The Subsonic Mach Number Correction. Cascade tests in the decades following the publication of the AMDC loss system have revealed that the profile loss coefficient Y_p is in general not independent of Mach number, even in the subsonic flow regime. Compressibility can affect Y_p in two ways, by causing shocks at blade leading edges and by affecting the flow acceleration within blade channels.

Shock Loss. Shocks at blade leading edges can set in at relatively low average inlet Mach number levels, due to the local flow acceleration adjacent to the highly curved leading edges. Evidence of the possible detrimental effects of this can be deduced from design rules of bygone days, which warn us about designing for relative inlet Mach numbers greater than approximately 0.6, and admonish us to design thinner leading edges when inlet Mach numbers are high.

Due to the radial variation in gas conditions, necessary for the flow to be in equilibrium, incident Mach numbers are always higher at the hub than at midspan. A sampling of known turbines resulted in the curve shown in Fig. 6, which estimates the incident Mach number at the hub of nonfree-vortex turbine blades when midspan Mach number and hub/tip radius ratio are known. The "shock loss" next to the
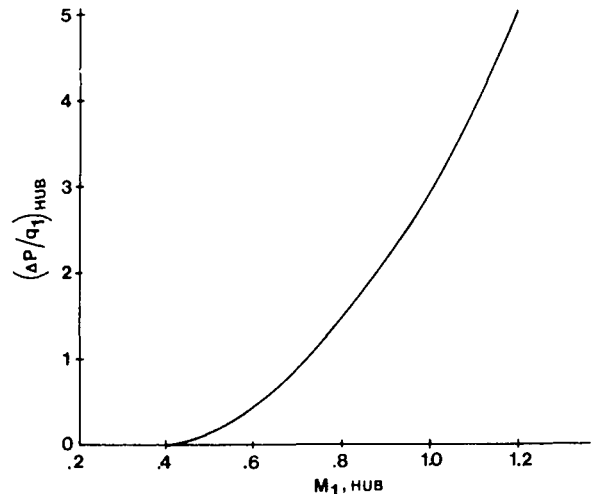
inner endwall of a blade can then be found from Fig. 7, which states

$$\left.\frac{\Delta P}{q_1}\right)_{HUB} = 0.75(M_{1,HUB} - 0.4)^{1.75} \tag{4}$$

However, since this loss is only local, it would be unfair to penalize the whole blade by this amount: a long blade would be less affected, overall, by a loss here than would a short blade. Therefore, the contribution to the mean line loss of blade inlet shock losses is taken to be

$$\left.\frac{\Delta P}{q_1}\right)_{SHOCK} = \left(\frac{R_H}{R_T}\right)\left(\frac{\Delta P}{q_1}\right)_{HUB} \tag{5}$$

Finally, the subsonic shock loss coefficient, until now expressed in terms of blade inlet mean line dynamic head, can be expressed in terms of blade exit dynamic head by

$$\left.\frac{\Delta P}{q_2}\right)_{SHOCK} \equiv Y_{SHOCK} = \left.\frac{\Delta P}{q_1}\right)_{SHOCK} \left(\frac{p_1}{p_2}\right)$$

$$\frac{1 - \left(1 + \frac{\gamma-1}{2}M_1^2\right)^{\frac{-\gamma}{\gamma-1}}}{1 - \left(1 + \frac{\gamma-1}{2}M_2^2\right)^{\frac{-\gamma}{\gamma-1}}} \tag{6}$$

Channel Flow Acceleration. Flow in the passage formed by two adjacent blades will undergo a larger velocity change when operated at a higher (subsonic) Mach number level. This is a consequence of the compressibility of the working
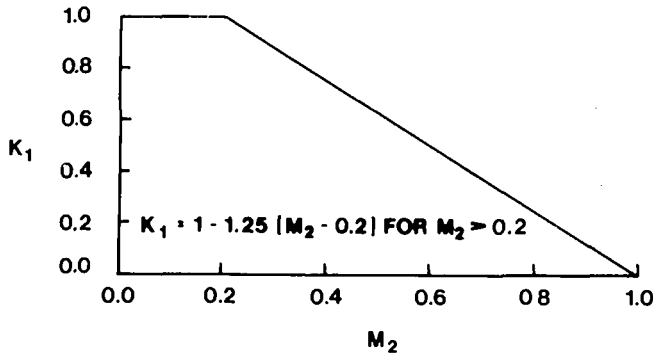
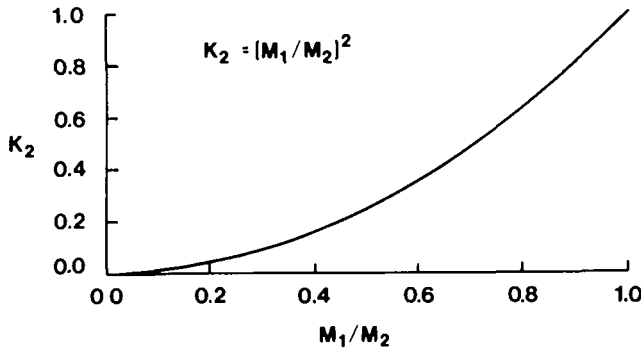Fig. 8 Mach number correction factor K_1 for the profile loss coefficient, for accelerating cascades of $M_1 \rightarrow M_2$

Fig. 9 Mach number correction factor K_2 for the profile loss coefficient

Fig. 10 Comparison of transonic cascade test results with prediction, blade profile 23

medium. In an accelerating flow passage, therefore, operation closer to sonic exit velocities will tend to cause suppression of local separations and the thinning of boundary layers. This effect is most pronounced where inlet Mach numbers are only slightly lower than exit Mach numbers.

Profile loss coefficients shown in Figs. 1 and 2 are derived from cascade tests carried out at low subsonic velocities and are therefore pessimistic when applied to turbines operating at higher Mach number levels. Figures 8 and 9 correct for the effects of exit Mach number and channel acceleration, respectively. The combined effect of these corrections is

$$K_P = 1 - K_2(1 - K_1) \qquad (7)$$

In the subsonic regime of operation of a cascade of blades, therefore, the profile loss coefficient Y_P becomes:

$$Y_P = 0.914 \left(\frac{2}{3} Y_{P,\text{AMDC}} K_P + Y_{\text{SHOCK}} \right) \qquad (8)$$

As discussed in the forthcoming section, "Verification of Loss System," these compressibility corrections were necessary to make the AMDC loss system predict the correct shapes of the efficiency islands on "Smith's chart."

Supersonic Drag Rise. In the regime of supersonic exit velocities additional pressure losses occur as a result of shocks originating in the trailing edge wake. Due to the lack of cascade test results of adequate quality, a reliable loss model is not yet available.

The AMDC loss system assumes a supersonic drag rise according to

$$\text{CFM} = 1 + 60(M_2 - 1)^2 \qquad (9)$$

where CFM is applied as a multiplier to Y_P, when the exit Mach number exceeds unity. This factor is taken to be independent of blade (metal) exit angle. This assumption ap-
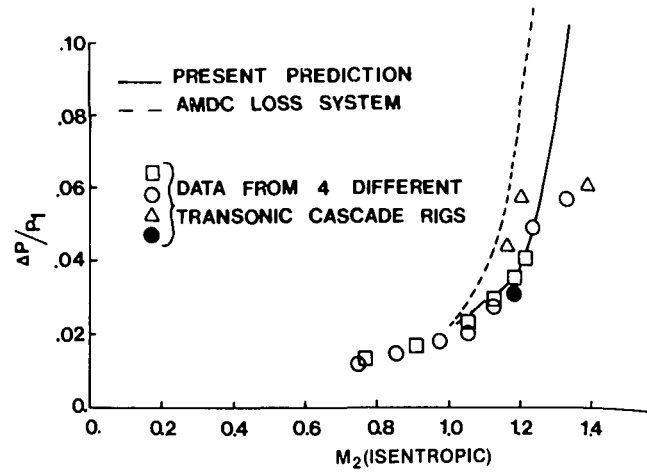
pears to be the major shortcoming of this correction in that it ignores limit loading of airfoils.

Limit load is the condition at which a given cascade of airfoils operating at a constant inlet pressure develops maximum tangential force. When blade trailing edges are more tangential, this condition occurs at a higher Mach number, and therefore different cascades will have different limit load exit Mach numbers. Limit load Mach number can be estimated from blade geometry [6,7], but it can also be predicted from supersonic drag rise, if that is known [8]. Alternatively, the supersonic drag rise may be deduced from known limit load Mach number calculated from blade geometry. Work on this approach is currently in progress. Early results look promising as shown in Fig. 10. This regime is as yet primarily of interest for efficiency prediction at off-design operating conditions, however. Design point exit Mach numbers of turbines in current gas turbine engines rarely assume magnitudes where supersonic drag rise plays a significant part in the loss system.

Reynolds' Number Correction. It is assumed that the profile loss coefficient Y_P is calculated at a reference Reynolds' number of 2×10^5, based on true chord, and cascade exit gas conditions. At any other Reynolds' number, the correction $f_{(\text{Re})}$ in equation (1) is

$$
f_{(\text{Re})} = \left(\frac{\text{Rec}}{2 \times 10^5} \right)^{-0.4} \text{ for } \text{Rec} \leq 2 \times 10^5 \\
= 1.0 \text{ for } 2 \times 10^5 < \text{Rec} < 10^6 \\
= \left(\frac{\text{Rec}}{10^6} \right)^{-0.2} \text{ for } \text{Rec} > 10^6 \qquad (10)
$$

This formulation is similar but not identical to Denton's [9]. It is applied to the profile loss coefficient only as there is little evidence in the literature that other loss terms are affected. The Reynolds' number independence in the 2×10^5 to 10^6 range is an approximation to the complex loss coefficient variation in the transitional regime. The true variation of loss coefficient with Reynolds' number cannot be estimated without a detailed knowledge of blade shapes.

The Secondary Loss Coefficient Y_S

The secondary loss coefficient calculation is the same as given by Dunham and Came [5], except for its dependence on blade aspect ratio. In [5] it is assumed that Y_S varies as the
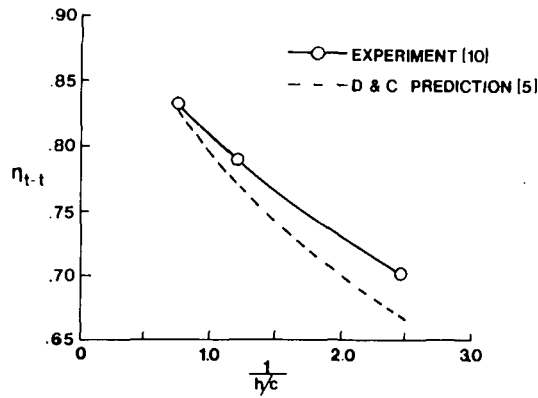
Fig. 11 Comparison of the effect of blade aspect ratio as predicted by the Dunham and Came method [5] with the test results of Rogo [10]

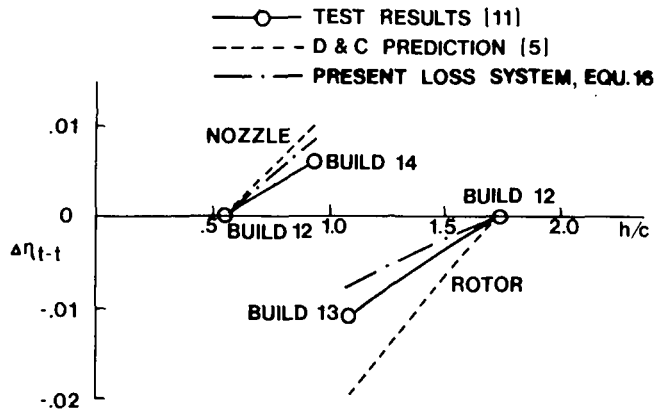Fig. 13 Mach number correction factor K_3 for the secondary loss coefficient

Fig. 12 Comparison of the effect of blade aspect ratio as predicted by Dunham and Came [5] and the present method, with the test results of Okapuu [11]

reciprocal of blade aspect ratio, over the complete range of aspect ratios. Its authors noted that their method predicted a more rapid increase in losses, as aspect ratio was reduced, than shown by the experimental data of Rogo [10], Fig. 11. The same trend has been confirmed by the data of Okapuu [11]. In the present loss system this rise in Y_S (with a reduction in aspect ratio) is less rapid for aspect ratios less than two. The following equations are employed:

$$Y_{S,AMDC} = 0.0334 f_{(AR)} \left(\frac{\cos\alpha_2}{\cos\beta_1} \right) \left(\frac{C_L}{s/c} \right)^2 \frac{\cos^2\alpha_2}{\cos^3\alpha_m} \qquad (11)$$

where

$$\frac{C_L}{s/c} = 2(\tan\alpha_1 + \tan\alpha_2)\cos\alpha_m \qquad (12)$$

$$\alpha_m = \tan^{-1}\left[\frac{1}{2}(\tan\alpha_1 - \tan\alpha_2) \right] \qquad (13)$$

$$f_{(AR)} = \frac{1 - 0.25\sqrt{2 - h/c}}{h/c} \quad \text{for } h/c \leq 2$$

$$= \frac{1}{h/c} \qquad \text{for } h/c > 2 \qquad (14)$$

Figure 12 shows the effect of aspect ratio on predicted turbine efficiency. The modification introduced here is seen to provide a better prediction of test results.

In the AMDC loss system, Y_S given by equation (11) is multipled by Y_{TET}. However, in the present loss system the
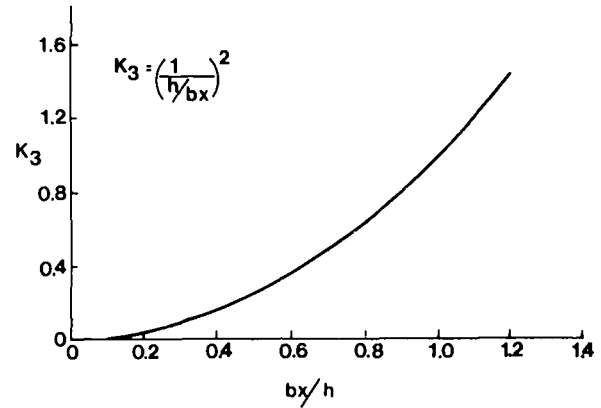
secondary losses and the trailing edge losses are not linked. Therefore, it is required that Y_S, as given by equation (11), should be suitably modified before it can be used in the present loss system. This is done by multiplying Y_S (equation (11)) by a factor of 1.2. An initial estimate for the multiplying factor was based on the assumption that Dunham and Came [5] developed their loss system for turbines having a typical value of $t/o \simeq .1$ and an airfoil gas exit angle of 60 deg. This implied that their turbines had $t/s \simeq .05$. In the AMDC loss system, for $t/s \simeq 0.05$, the value of Y_{TET} is not much different from 1.2. The value of the multiplying factor was further confirmed by optimisation of the present loss system performance (to be discussed later).

The Subsonic Mach number Correction. As with profile losses, compressibility also has an effect on the acceleration of flow next to endwalls, and hence endwall losses. To account for this the subsonic Mach number correction factor for secondary losses is defined in terms of the factor for profile loss and aspect ratio as

$$K_s = 1 - K_3(1 - K_P) \qquad (15)$$

where K_3 is defined in Fig. 13 and K_p as defined in equation (7). Leading edge shocks at high subsonic incident Mach numbers are also likely to have some effect on secondary losses. These effects are here assumed to be included in the term Y_{SHOCK}, equation (6), and not separately accounted for here. In the supersonic exit regime no additional Mach number correction is applied to Y_S, which is kept fixed at its value corresponding to exit Mach number of unity. Therefore:

$$Y_s = 1.2 Y_{S,AMDC} K_s \qquad (16)$$

The Trailing Edge Loss Coefficient Y'_{TET}

The physically most meaningful expression of pressure losses due to trailing edge blockage is in terms of trailing edge blockage itself, i.e., in terms of the trailing edge thickness/throat opening ratio of a cascade.

An extensive survey of published and in-house cascade results produced the relationship shown in Fig. 14. Trailing edge losses are here expressed in terms of an energy coefficient $\Delta\phi^2_{TET}$. Two distinct curves exist for axial entry nozzles and impulse blades. The difference lies in the thicknesses of profile boundary layers at the trailing edges of blades: impulse blades, with their thick boundary layers have lower (less negative) base pressure coefficients and thus have lower trailing edge losses, while the trailing edge thickness contributes significantly to the drag of highly accelerating cascades. For blades other than the two basic types shown,
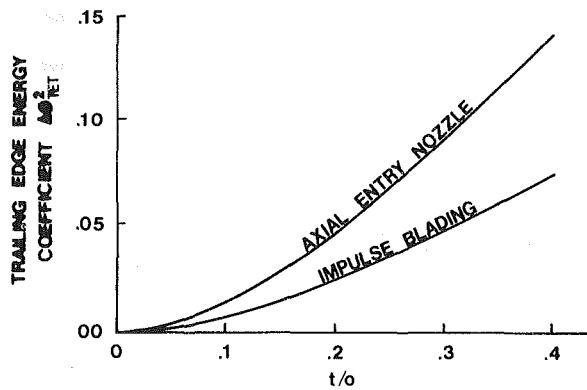
Fig. 14 Trailing edge loss [energy] coefficient correlated against the ratio of trailing edge thickness to throat opening

Fig. 15 Turbine stage efficiency at zero tip leakage, after Smith [12]

trailing edge losses are interpolated in a manner similar to equation (3), i.e.,

$$\Delta\phi^2_{TET} = \Delta\phi^2_{TET\,(\beta_1\,=0)}$$

$$+ \left|\frac{\beta_1}{\alpha_2}\right| \left(\frac{\beta_1}{\alpha_2}\right) \left[\Delta\phi^2_{TET\,(\beta_1\,=\,\alpha_2)} - \Delta\phi^2_{\text{TET}(\beta_1=0)}\right] \qquad (17)$$

The conversion from kinetic energy loss coefficient to pressure loss coefficient is given by

$$Y'_{TET} = \frac{\left[1 - \frac{\gamma-1}{2}M_2^2\left(\frac{1}{1-\Delta\phi^2_{TET}} - 1\right)\right]^{-\frac{\gamma}{\gamma-1}} - 1}{1 - \left(1 + \frac{\gamma-1}{2}M_2^2\right)^{-\frac{\gamma}{\gamma-1}}} \qquad (18)$$

The variation of Y'_{TET} with Mach number is not well documented at present. For supersonic exit velocities the supersonic drag rise, as discussed under profile losses, is assumed to include trailing edge losses.

The Tip Clearance Loss Coefficient Y_{TC}

Overtip leakage losses on unshrouded rotor blades constitute a major source of turbine inefficiency. A large body of experimental data exists on this subject, relating changes in turbine efficiency to changes in rotor tip clearance. Most of the available results correlated within ± 15 percent with the following expression:

$$\frac{\dfrac{\Delta\eta}{\eta_o}}{\dfrac{\Delta k}{h\,\cos\alpha_2} \times \dfrac{R_{\text{TIP}}}{R_{\text{MEAN}}}} = 0.93 \qquad (19)$$

When the loss system is structured as equation (1) $\Delta\eta$ has to be converted to an equivalent loss coefficient Y_{TC}. This may be done iteratively (by first calculating turbine efficiency with zero tip clearance, assessing the efficiency penalty due to clearance and increasing the rotor loss coefficient until the process converges on efficiency, all the while recalculating the velocity triangles and other loss coefficients) or directly, by making certain simplifying assumptions. The exact process is beyond the scope of this paper.

In the case of shrouded turbine blades the loss system incorporates the relationship proposed in [5], i.e.

$$Y_{TC} = 0.37\frac{c}{h}\left(\frac{k'}{c}\right)^{0.78}\left(\frac{C_L}{s/c}\right)^2 \frac{\cos^2\alpha_2}{\cos^3\alpha_m} \qquad (20)$$

where

$$k' = \frac{k}{(\text{number of seals})^{0.42}} \qquad (21)$$

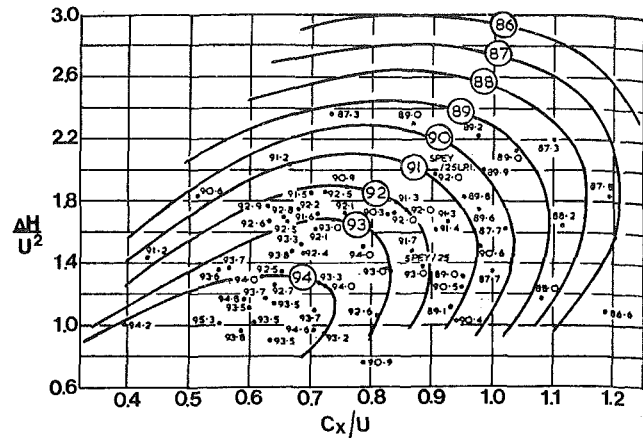The reason for deviating from the AMDC loss system in the

case of unshrouded blades was that tip leakage losses were found to be overpredicted by that system on recent turbines.

Verification of Loss System

The loss system outlined in the foregoing evolved to its final formulation largely thanks to a 1965 paper by Smith [12], which proposes a correlation of turbine efficiency on a "loading diagram" having stage loading factor $\Delta H/U^2$ as one axis and stage flow factor Cx/U as the other (Fig.15). Design point efficiencies (corrected to zero tip clearance) of some 69 turbines, plotted on this diagram, strongly suggest concentric locii of constant efficiency. This correlation is so convincing that it must be accepted as one of the tests which any mean line loss system must satisfy.

These 69 turbines were, clearly, all designed before 1965. In addition they all share certain common design features described in [12], features which are a reflection of the consistent design philosophy in the organization whence they originated. Considering the probable sizes of these turbines, the state of the (design) art at the time and the manner of testing, one arrives at the conclusion that the efficiency contours shown in Fig. 15 are caused mainly by profile losses and somewhat more weakly (due to the prevailing moderate to large aspect ratios) by secondary losses. Therefore, if a candidate loss system fails to duplicate the Smith's chart, the fault is likely to lie with its profile and/or secondary loss components.

To test these loss system components, the equivalent of 103 turbine stages were designed, using design rules and mechanical limitations current in the 1950's. As a guide, multistage turbine gas paths and approximate cycle design points of three engines of this period were used as a framework for these stages. The design point efficiency of each was then calculated by a candidate loss system and a plot similar to the Smith's chart was constructed.

The Ainley/Mathieson loss system, while predicting quite well the variation of efficiency with $\Delta H/U^2$, failed to adequately predict its variation with Cx/U at Cx/U values in excess of 0.6. In this respect our results were quite similar to those of Amann and Sheridan [13]. After examining various alternatives we were forced to conclude that only the compressibility and shock loss corrections to profile and secondary loss coefficients, described in the foregoing, can produce an adequate simulation of Smith's chart. It was found that the shock loss correction (Y_{SHOCK}) mainly affected the high Cx/U regime of the chart, while the acceleration correction (K_p) affected the general level of the efficiency contours. Figures 6, 7, 8, 9 and 13 were evolved by trial and error until a simulation of Smith's curves was obtained. The
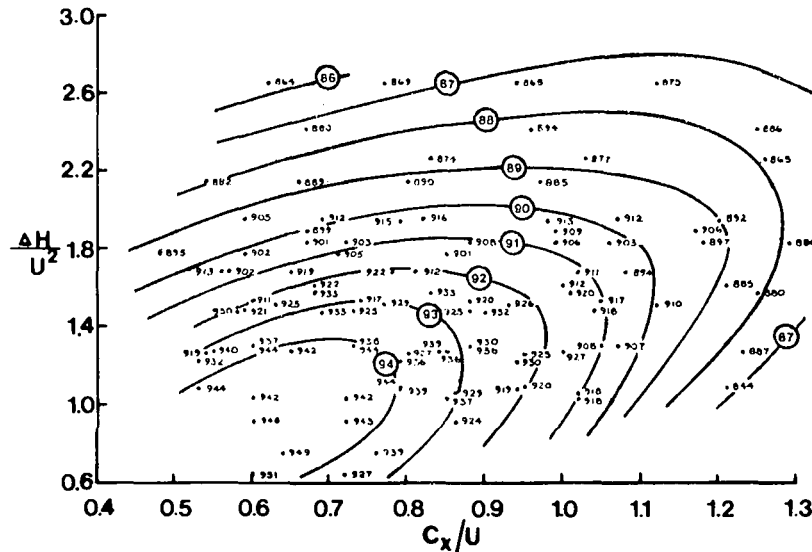
Fig. 16 Turbine stage efficiency at zero tip leakage calculated by the present method
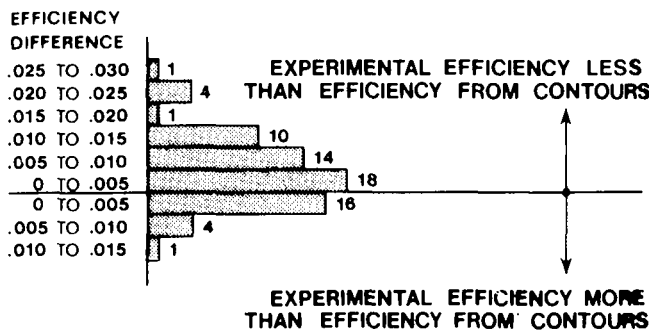
EFFICIENCY
DIFFERENCE

EXPERIMENTAL EFFICIENCY LESS THAN EFFICIENCY FROM CONTOURS

.025 TO .030	1
.020 TO .025	4
.015 TO .020	1
.010 TO .015	10
.005 TO .010	14
0 TO .005	18
0 TO .005	16
.005 TO .010	4
.010 TO .015	1

EXPERIMENTAL EFFICIENCY MORE THAN EFFICIENCY FROM CONTOURS

Fig. 17 Histogram for experimental data used to define contours in Fig. 15, after Amann and Sheridan [13]

EFFICIENCY
DIFFERENCE

CALCULATED EFFICIENCY LESS THAN EFFICIENCY FROM CONTOURS

.025 TO .030	1
.020 TO .025	
.015 TO .020	
.010 TO .015	8
.005 TO .010	10
0 TO .005	31
0 TO .005	24
.005 TO .010	19
.010 TO .015	9
.015 TO .020	1

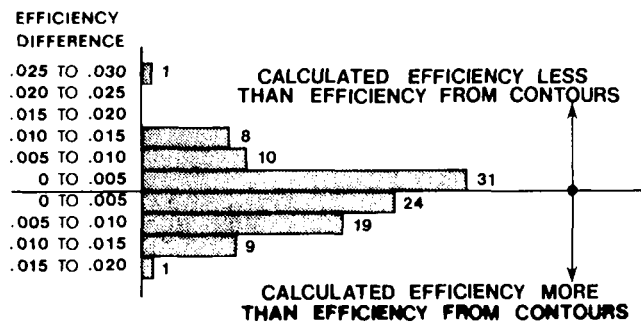CALCULATED EFFICIENCY MORE THAN EFFICIENCY FROM CONTOURS

Fig. 18 Histogram for calculated data used to define contours in Fig. 16

result is shown in Fig. 16. Calculations were carried out with the whole AMDC value of Y_P (rather than 2/3) in equation (8) to simulate the state of blade design art of the time.

A qualitative comparison of Figs. 15 and 16 indicates that a satisfactory duplication of the shapes of efficiency contours has been achieved. At low values of $\Delta H/U^2$ there is unquestionably an initial increase in efficiency with $\Delta H/U^2$, at constant Cx/U. The lack of this feature has been the major shortcoming of the AMDC loss system as demonstrated in Fig. 9 of [13].

Quantitatively, Fig. 16 differs from Fig. 15 in that a given efficiency curve of Fig. 16 attains a lower peak $\Delta H/U^2$ value but extends to a higher peak Cx/U value. At 90 percent efficiency, for example, the maximum discrepancy amounts to 1½ efficiency points in each regime, while at 94 percent the discrepancy is ½ efficiency point. This is partly explained by an examination of the data from which efficiency contours were derived. Figure 17 describes the differences between data points and contours of Fig. 15, as reported in [13]. It is clear that a considerable uncertainty exists in the positioning of efficiency contours. It is also evident that a bias exists in the contours, which are predicting efficiencies approximately ½ point higher than supported by data points. This would tend to reduce the discrepancy between Figs. 15 and 16, at peak $\Delta H/U^2$. As to the region of peak Cx/U, Fig. 15 has too few data points at $Cx/U > 1.0$ to substantiate the curves drawn. Unpublished test data from other sources suggest that these curves may in fact extend to higher Cx/U, as in Fig. 16. These

speculations aside, the quantitative agreement may nevertheless be considered satisfactory in the light of the inevitable data scatter inherent in both figures. Figure 18 shows the corresponding differences between data points and contours of Fig. 16, for completeness.

The second test of a loss system is the demonstration of its ability to predict the design point efficiencies of existing turbines of more recent vintage. Design point data were collected for 33 turbines ranging from the gas generator turbine of a small automobile engine to the low pressure turbine of a 45,000-lb thrust turbofan. In view of the advances made in blade profile design over the last 25 yr, the loss system was operated with only 2/3 of the AMDC profile loss coefficient. Since none of these turbines had bladerow exit Mach numbers in excess of 1.17 the supersonic drag rise correction (by the present prediction, Fig. 10) had only a small effect on the efficiencies of transonic stages. Figure 19 shows the comparison. The closed symbols describe P&WA turbines. The open symbols describe turbines from other sources. Table 1 lists the more important design parameters of these turbines.

The agreement is generally very good, the majority of predictions falling within an error band of 1½ efficiency points. Of the few turbines which fall significantly outside this error band two can readily be shown to be "incompetent" designs, and the experimental techniques used in the case of two more are open to criticism.

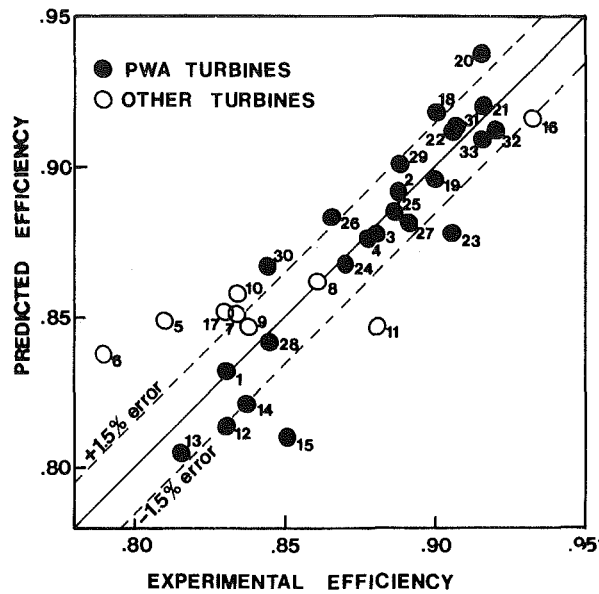Figure 20 shows an identical comparison of the same 33

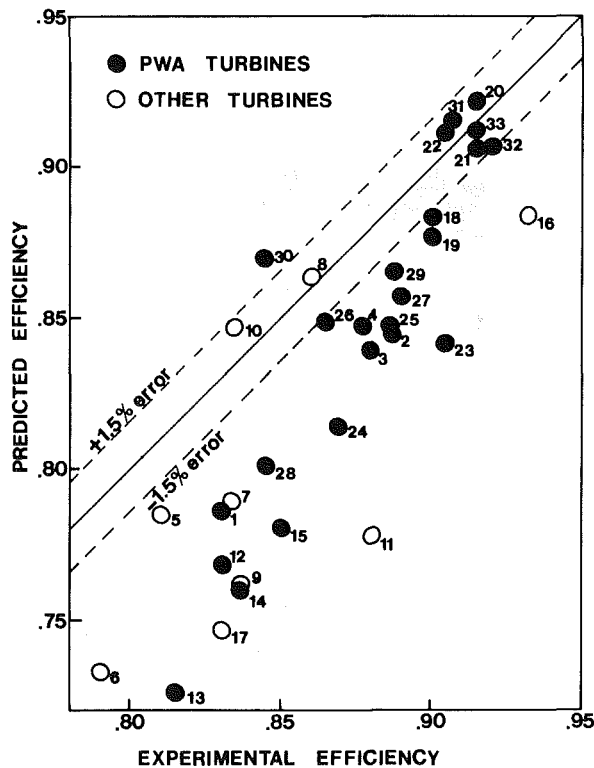Fig. 19 Comparison of predicted efficency with experimental efficiency of 33 turbines (new loss system)

Fig. 20 Comparison of predicted efficiency with experimental efficiency of 33 turbines (AMDC loss system)

turbines carried out with the AMDC loss system. The agreement is not satisfactory.

The design point efficiencies under discussion here are those obtainable on rotating aerodynamic rigs. In the engine environment these turbines will generally show a lower efficiency for a variety of reasons such as effects of secondary air injection, leakages, nonuniformities in the turbine inlet flow, etc. These features are not accounted for the in the loss system described in the foregoing. Also not accounted for are the inevitable future advances in the art of turbine design:

NO.	SOURCE	# STAGES	STAGE	$\Delta H/U^2$	Cx/U	PRESS. RATIO	$\overline{h/c}$ NOZZLE	$\overline{h/c}$ ROTOR
1	P&WA	1	1	1.88	.54	2.67	.366	1.75
2	P&WA	1	1	1.51	.533	4.00	.612	1.98
3	P&WA	1	1	1.45	.565	3.89	.571	1.72
4	P&WA	1	1	1.55	.570	2.95	.437	2.188
5	OTHER	1	1	1.25	.613	2.98	.520	.671
6	OTHER	1	1	1.55	.675	2.90	.55	.825
7	OTHER	1	1	1.59	.642	2.90	.725	1.26
8	OTHER	1	1	1.11	.383	1.48	1.50	1.50
9	OTHER	1	1	1.656	.595	2.77	1.0	1.0
10	OTHER	2	1	.989	.309	1.11	1.44	1.456
			2	.987	.318	1.11	1.32	1.489
11	OTHER	1	1	1.672	.696	1.82	.71	1.01
12	P&WA	1	1	1.19	.397	2.00	.317	.739
13	P&WA	1	1	1.19	.531	2.00	.247	.777
14	P&WA	1	1	1.19	.497	2.00	.253	.670
15	P&WA	1	1	1.139	.322	3.40	.24	.486
16	OTHER	2	1	1.65	.690	1.71	1.47	1.87
			2	1.65	.813	1.87	1.54	2.16
17	OTHER	1	1	2.00	.721	1.99	.468	.847
18	P&WA	1	1	1.44	.566	2.76	.637	1.9
19	P&WA	2	1	1.50	.924	1.45	1.27	2.09
			2	1.77	.990	1.65	1.95	2.47
20	P&WA	2	1	.9	.622	1.44	1.102	2.23
			2	.83	.502	1.53	1.81	3.02
21	P&WA	2	2	1.28	.758	1.70	1.102	2.23
			1	1.02	.698	1.73	1.81	3.02
22	P&WA	1	1	1.94	.529	2.24	1.23	2.67
23	P&WA	1	1	2.388	.712	2.68	1.23	2.67
24	P&WA	1	1	1.45	.565	3.89	.571	1.08
25	P&WA	1	1	1.45	.561	3.89	.984	1.72
26	P&WA	1	1	1.516	.583	2.81	.421	1.95
27	P&WA	1	1	1.463	.492	3.23	.527	2.155
28	P&WA	1	1	1.38	.485	1.99	.710	.921
29	P&WA	1	1	1.58	.545	1.94	1.328	1.111
30	P&WA	4	1	2.44	1.50	1.33	2.61	3.94
31	"		2	2.32	1.28	1.35	4.07	4.98
32	"		3	2.38	1.25	1.45	5.01	5.76
33	"		4	2.71	1.50	1.68	5.68	5.80

novel techniques to minimize overtip leakage losses and fully three-dimensional flow analysis methods are already showing promise of a bright future.

A mean line efficiency prediction method is the sum of a large number of loss components. While some of them may prove to be quantitatively imperfect, the manner in which they are combined may cause errors to cancel. The final proof of a loss system must be its ability to correctly predict the efficiencies of well documented turbines.

Conclusion

Regardless of the degree of sophistication of analytical tools available for the detail design of turbine blading, a mean line design technique will always be needed for the optimization of the turbine gas path and the prediction of attainable turbine efficiency of a new engine.

The mean line loss system described, a development of the Ainley/Mathieson/Dunham/Came system, appears to be capable of predicting design point efficiencies of current turbines of conventional stage loadings and "competent" design to within ± 1½ efficiency points. A major departure from AMDC is the restructuring of the loss system and the introduction of compressibility effects and shock losses into the calculation of profile and secondary loss coefficients.

Acknowledgments

References

1 Traupel, W., "Thermische Turbomaschinen," Springer-Verlag, Berlin, 1966.

2 Craig, H.R.M., and Cox, H.J.A., "Performance Estimate of Axial Flow Turbines," *Proceedings of the Institution of Mechanical Engineers*, Vol. 185, No. 32, 1971, pp. 407–424.

3 Stewart, W.L., "A Study of Axial Flow Turbine Efficiency Characteristics in Terms of Velocity Diagram Parameters," ASME Paper No. 61-WA-37, 1961.

4 Ainley, D.G., and Mathieson, G.C.R., "A Method of Performance Estimation for Axial Flow Turbines," British ARC, R&M 2974, 1951.

5 Dunham, J., and Came, P.M., "Improvements to the Ainley/Mathieson Method of Turbine Performance Prediction," ASME JOURNAL OF ENGINEERING FOR POWER, July 1970, pp. 252–256.

6 Hauser, C., and Plohr, H.W., "Two-Dimensional Cascade Investigation of the Maximum Exit Tangential Velocity Component and Other Flow Conditions at the Exit of Several Turbine Blade Designs at Supercritical Pressure Ratios," NACA RME51F12, Aug. 1951.

7 Fruchtman, I., "The Limit Load of Transonic Turbine Blading," ASME Paper No. 74-GT-80, Apr. 1974.

8 Okapuu, U., "Limit Load and Supersonic Drag Rise of Transonic Turbine Cascades," Pratt & Whitney Aircraft of Canada, Internal Memo, July 1974.

9 Denton, J.D., "A Survey and Comparison of Methods for Predicting the Profile Loss of Turbine Blades," Institute of Mechanical Engineers Conference Publication 3, Paper C76/73, 1973, pp. 204–212.

10 Rogo, C., "Experimental Aspect Ratio and Tip Clearance Investigation on Small Turbines," SAE Paper 680448, Mid Year Meeting Detroit, Mich., May 20–24, 1968.

11 Okapuu, U., "Some Results from Tests on a High Work Axial Gas Generator Turbine," ASME Paper No. 74-GT-81, Apr. 1974.

12 Smith, S.F., "A Simple Correlation of Turbine Efficiency," *Journal of Royal Aeronautical Society*, Vol. 69, July 1965, pp. 467–470.

13 Amann, C.A., and Sheridan, D.C., "A Comparison of Some Analytical and Experimental Correlations of Axial Flow Turbine Efficiency," ASME Paper No. 67-WA/GT-6, Nov. 1967.